POSTCRITICAL IMPERFECTION-SENSITIVE BUCKLING AND OPTIMAL BRACING OF LARGE REGULAR FRAMES

By Zdeněk P. Bažant,[1] Fellow, ASCE, and Yuyin Xiang[2]

ABSTRACT: Periodic interior buckling of regular multistory and multibay rectangular elastic frames with elastic bracing is analyzed. It is shown that there exists a certain critical bracing stiffness for which the critical loads for the nonsway (symmetric) and sway (antisymmetric) buckling modes coincide. Simple formulae for the critical stiffness are given. For the critical and softer bracing, the type of postcritical buckling behavior is the unstable symmetric bifurcation, exhibiting imperfection sensitivity according to Koiter's 2/3-power law. For stiffer bracing, there is no imperfection sensitivity. The critical bracing, however, represents a naive optimal design which should be avoided because the imperfection sensitivity is the strongest. It is recommended that the truly optimal bracing should be significantly stiffer (perhaps 1.1 to 2 times as stiff). The buckling behavior, including the postcritical imperfection sensitivity, is similar to that of a portal frame analyzed before. The solution also provides a demonstration of a simple method for the initial postcritical analysis of frames recently proposed by Bažant and Cedolin, which is based on energy minimization. In this method, the distribution of cross section rotations is assumed to be the same as in the classical linearized theory. The curvatures and deflections are obtained from the rotations by integration with at least a second-order accuracy (in terms of the rotations), and the axial shortening with at least a fourth-order accuracy.

INTRODUCTION

The design of slender columns and frames is currently based on the critical load for elastic buckling and on the magnification factor for the initial bending moment derived from the critical load. Such analysis, however, does not provide uniform safety factors for columns or frames of different types. Some columns and frames exhibit symmetric stable bifurcation, which is imperfection insensitive. Others exhibit unstable symmetric bifurcation or asymmetric bifurcation, which are both imperfection sensitive, the latter more than the former. This sensitivity, which means that imperfections cause the maximum load to be less than the critical load, is generally described by Koiter's asymptotic theory of initial postcritical behavior (Koiter 1945, 1967; Koiter and Kuiken 1971; Thompson and Hunt 1973; Hutchinson and Koiter 1970; Budianski 1974; Brush and Almroth 1975; Kollár and Dulácska 1984; Thompson and Hunt 1984; Bažant and Cedolin 1989, 1991).

For shells, Koiter's theory has been extensively applied and has become well established. For columns and frames, however, it has not been applied in practice and has not found its way into the building codes. The reason of course is that columns and frames are much less imperfection-sensitive than shells. In shells, inevitable random imperfections may cause the maximum load to be 60–80% less than the theoretical critical load of a perfect shell. In columns and frames, this reduction can hardly exceed 10%. Such inaccuracy is perhaps practically tolerable, in view of the large safety factors used. But it means that for some types of frames the true safety factor is typically 5–10% smaller than for others [as for example demonstrated for an L-shaped frame by Roorda (1965a,b), Roorda (1968), Roorda and Chilver (1970), Koiter (1967), Kounadis (1985), and Bažant and Cedolin (1989)]. This is not an ideal state of affairs, especially since it is not difficult, and with a computer in fact very easy, to take the different imperfection sensitivities of various types of frames into account.

Experience shows that, for rectangular frames, the nonsway (symmetric) buckling mode usually exhibits stable symmetric bifurcation, which is imperfection insensitive. On the other hand, the sway (asymmetric) mode of buckling has been shown for some rectangular frames to be imperfection sensitive. For example, as shown by Koiter (1967), the L-frame exhibits asymmetric bifurcation, which is strongly imperfection sensitive, following Koiter's 1/2-power law (Koiter 1945) according to which the imperfection causes the maximum load to decrease as the 1/2-power of the imperfection (see also Roorda 1965a,b; Kounadis et al. 1977; Bažant and Cedolin 1989; Bažant and Cedolin 1991, section 2.6). The portal frame, whose bifurcation behavior was studied by von Mises and Ratzendorfer (1926), Chwalla (1938), Bažant (1943), Bleich (1961), Timoshenko and Gere (1961), and Britvec (1973), was shown by Kounadis (1983) and Simitses et al. (1981) to exhibit unstable symmetric bifurcation. This bifurcation is imperfection sensitive but not as strongly as the asymmetric bifurcation exhibited by the L-frame. It follows Koiter's 2/3-power law (Koiter 1945), according to which the imperfection causes the maximum load to decrease as the 2/3-power of the imperfection. Practically an important type of buckling is the periodic interior buckling of braced and unbraced regular multibay and multistory rectangular frames. It seems that their postcritical imperfection sensitivity has not yet been examined. This will be the objective of this paper.

The second objective will be to examine from the design viewpoint the effect of elastic bracing on the imperfection sensitivity of the aforementioned interior buckling. As shown by Kounadis (1983), if the stiffness of the bracing of a symmetric portal frame is less than a certain critical value, the critical load for the sway buckling mode of the braced portal frame becomes less than the critical load for the nonsway mode, and in that range of bracing stiffness the buckling is imperfection sensitive according to the 2/3-power law. It follows that the bracing of a stiffness lower than this critical value should be avoided in design. It will be shown here that a similar behavior is exhibited by the interior buckling of large regular frames.

For a certain bracing stiffness, the sway and nonsway buckling loads of the portal frame coincide (Kounadis 1983). From the viewpoint of critical load, this represents the optimal design. However, as experience shows, coincidence of the critical loads of two different buckling modes increases the imperfection sensitivity. Thus, if the postcritical imperfection sensitivity is taken into account, one finds that the aforementioned bracing design is in fact not optimum. Therefore, such a design

[1]Walter P. Murphy Prof. of Civ. Engrg and Mat. Sci., Northwestern Univ., Evanston, IL 60208.

[2]Grad. Res. Asst., Northwestern Univ., Evanston, IL.

Note. Associate Editor: Eric M. Lui. Discussion open until September 1, 1997. To extend the closing date one month, a written request must be filed with the ASCE Manager of Journals. The manuscript for this paper was submitted for review and possible publication on January 26, 1996. This paper is part of the ***Journal of Structural Engineering***, Vol. 123, No. 4, April, 1997. ©ASCE, ISSN 0733-9445/97/0004-0513–0522/$4.00 + $.50 per page. Paper No. 12476.

is called the "naive" optimum design (e.g., Bažant and Cedolin 1991). Naive optimal designs have been demonstrated for box girders with wall stiffeners and for latticed columns, in which the naive optimum design is obtained when the critical loads for the local and global buckling coincide. In the case of the portal frame, the naive optimal design is obtained for the bracing stiffness for which the critical loads of the sway and nonsway buckling modes coincide. This paper will answer the question of naive optimal design for the interior buckling of a large regular frame.

The analysis that follows will use a new efficient method of initial postcritical analysis proposed by Bažant and Cedolin (1991, section 5.9), which is based on assuming the distribution of the rotations along the beam-column to have the same form as in the classical linear analysis of critical load.

PROBLEM DEFINITION AND CONSEQUENCES OF PERIODICITY

Large frames give rise to a large number of unknowns, requiring large-scale computer analysis which does not lend itself to easy understanding of the basic trends. Large rectangular frames, however, are often regular or almost regular, and exhibit periodic buckling modes. The regularity and periodicity may be exploited to reduce the number of unknowns greatly and thus make simple, transparent, and easily interpretable solutions possible.

Consider a large multibay and multistory regular rectangular frame whose interior portion is shown in Fig. 1(a). The vertical axial forces in the columns vary from floor to floor: however, if the frame is very tall, then the change of axial force from one floor to the next is so small that a locally constant value of axial load P may be assumed. Similarly, the changes in the dimensions of the columns and beams from floor to floor may be neglected. Let l_c = height of the columns; EI_c = their bending stiffness; l_b = span of the beams; EI_b = their bending stiffness; and C_B = shear stiffness of the bracing of the whole floor. For steel frames, E = Young's modulus of material, and I_b, I_c = centroidal moments of inertia of cross sections, but for concrete frames the effective bending stiffness that takes into account the effect of cracking of concrete should be used. If n = number of columns in a floor, then $C_b = C_B/n$ = shear stiffness of the bracing per column.

We are interested in the interior buckling of the frame for which interactions with the boundaries of the frame are negligible. For this purpose, we may treat the regular frame as infinite. The only possible deflection pattern is periodic in horizontal as well as vertical direction [Fig. 1(b, d)]. The periodicity greatly reduces the number of unknown joint rotations and displacements. It suffices to analyze only the buckling of one cell consisting of a column, a beam, and a horizontal spring of stiffness C_b which simulates the stiffness of bracing per column; see Fig. 1(c, e) in which m_c and m_b are the moments due to buckling, transmitted from the neighboring column and beam. A column or beam far away from this cell may have rather different dimensions and axial load, but its interaction with the cell is negligible if it lies far enough.

The potential energy Π of this cell may be written as

$$\Pi = U - W, \quad U = U_c + U_b + U_e \tag{1}$$

in which W = work done by the applied load; U = strain energy stored; U_c, U_b, U_e = strain energies of the column, beam, and elastic spring that represent the bracing; subscripts c, b, e refer to the column, the beam, and the elastic bracing.

CRITICAL LOADS AND BUCKLING MODE OF PERFECT FRAME

Nonsway Buckling Mode

One periodic buckling mode of the infinite regular frame is the nonsway (symmetric) mode pictured, for the longest possible wavelength, in Fig. 1(b). In that case one needs to analyze only the cell in Fig. 1(c) because the deflections of the frame are periodic.

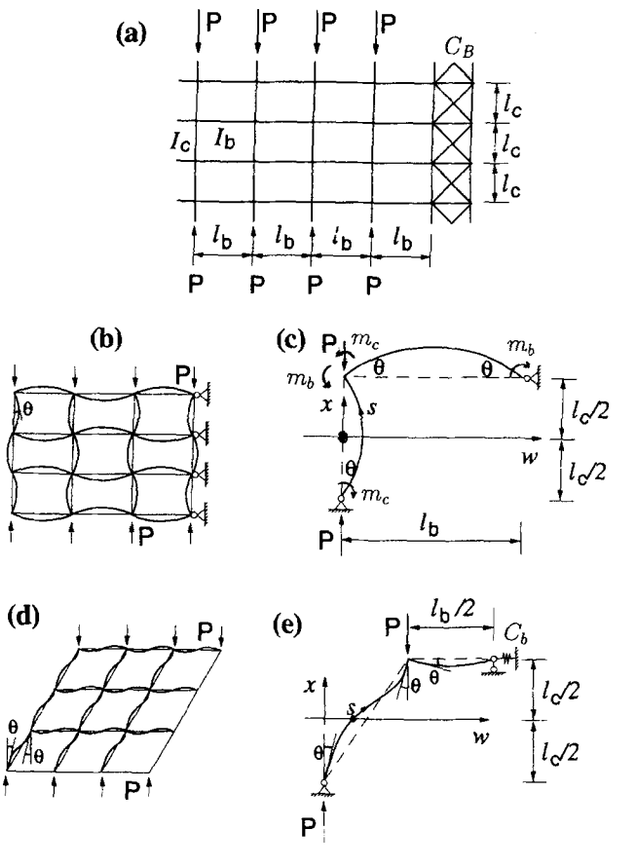

FIG. 1. (a) Large Regular Frame with Elastic Bracing; (b) Symmetric Buckling with (c) Its Basic Cell; (d) Antisymmetric Buckling with (e) Its Basic Cell

According to the linearized theory of buckling, the column deflection w has the general form $w = q_1 \sin kx + q_2 \cos kx + q_3 x + q_4$ where x = axial coordinate of the column; q_1, q_2, q_3, q_4 = constants to be determined from the boundary conditions; and $k = \sqrt{P/EI_c}$. Placing the origin of coordinate x (with the positive orientation upwards) at the midheight of the column, and imposing the boundary conditions at $x = \pm l_c/2$, one finds that

$$w = q[\cos(\lambda/2) - \cos kx] \tag{2}$$

in which q = arbitrary constant; and $\lambda = kl_c = l_c\sqrt{P/EI_c} = \pi\sqrt{P/P_E}$, in which $P_E = (\pi^2/l_c^2)EI_c$ = Euler load (critical load of pin-ended column). The end rotations are $\theta = -[w']_{x=l_c/2} = [w']_{x=-l_c/2} = qk\cos(\lambda/2)$. According to our definition of λ, the critical load of the frame is

$$P_{cr_1} = \lambda^2 EI_c/l_c^2 \tag{3}$$

where the subscript 1 refers to the nonsway (symmetric) buckling.

The quickest way to determine the critical loads of a perfect frame is to use the stiffness matrix of a beam-column involving the so-called stability functions; see, e.g., Bažant and Cedolin (1991, chapter 2) or Simitses (1976). Another way is the direct minimization of the quadratic expression for the potential energy. This way, briefly outlined in Appendix I, is more tedious, but also more direct. It relates more clearly to the postcritical analysis that follows, which is also based on minimization of the potential energy.

For the nonsway (symmetric) buckling of the frame, either of the two aforementioned methods yields the condition

$$\beta_b = -(\lambda/2)\cot(\lambda/2) \tag{4}$$

in which $\beta_b = (EI_b l_c)/(EI_c l_b)$ = parameter for the relative stiffness of the beams. For a given β_b, after solving λ from (4), we can calculate P_{cr} from (3). Because β_b is always nonnegative, $\lambda \geq \pi$ according to (4). Furthermore, for $\beta_b \to \infty$ we have $\lambda \to 2\pi$, according to (4). So, $\pi \leq \lambda \leq 2\pi$. This confirms for nonsway interior buckling of a regular rectangular frame the well-known condition

$$P_E \leq P_{cr_1} \leq 4P_E \tag{5}$$

Sway Buckling Mode

Another buckling mode of the infinite regular frame is the sway (antisymmetric) mode which is pictured, for the longest possible wavelength of the column, in Fig. 1(d), and for one cell in Fig. 1(e). The beam of the cell can be considered to have a hinged end at midspan [Fig. 1(e)] because there is an inflexion point at midspan, with no vertical deflection. Because of the antisymmetry of the buckling mode, $q_2 = 0$, and so $w = q_1 \sin kx + q_3(x/l_c) + q_4$. The boundary condition requires that $w = 0$ at $x = -l_c/2$ (column bottom), and so $q_4 = q_1 \sin(kl/2) + (q_3/2)$. Thus, the deflection of the column according to the linearized theory is:

$$w = q_1[\sin kx + \sin(\lambda/2)] + q_3[(x/l_c) + (1/2)] \tag{6}$$

where q_1, q_3 = displacement parameters. From this equation, we can express the rotations θ_1, θ_2 at the column ends and the horizontal displacement Δ at the column top.

Using either the stiffness matrix of a beam-column with the stability functions [e.g., Bažant and Cedolin (1991), chapter 2] or the direct minimization of the potential energy outlined in Appendix I, we obtain the following condition for the critical load for sway buckling:

$$\beta_e = \frac{\lambda^3[6\beta_b \cot(\lambda/2) - \lambda]}{6\beta_b[\lambda \cot(\lambda/2) - 2] - \lambda^2} \tag{7}$$

in which $\beta_e = (C_b I_c^3)/(EI_c)$ = parameter for the relative stiffness of bracing. For a given β_b and β_e, this equation gives λ, and thus the critical load according to (3).

For $\beta_e = 0$ (no bracing), the case $\beta_b \to 0$ implies that $\lambda \to 0$ or $P_{cr_2} \to 0$, and the case $\beta_b \to \infty$ implies that $\lambda \to \pi$ or $P_{cr_2} \to P_E$, where the subscript 2 refers to the sway (nonsymmetric) buckling. This confirms for the case of no bracing ($\beta_e = 0$) the well-known condition

$$0 \leq P_{cr_2} \leq P_E \tag{8}$$

Comparing this to (5), we also confirm that, if $\beta_e = 0$, P_{cr} for sway buckling cannot be larger than P_{cr} for nonsway buckling.

Coincidence of Critical Loads for Sway and Nonsway Modes

For bracing of nonnegligible stiffness ($\beta_e > 0$), P_{cr} for sway buckling can be larger than P_E. It can be even larger than P_{cr} for nonsway buckling. That this can indeed happen is confirmed by the plots of P_{cr_1}/P_E and P_{cr_2}/P_E versus β_b shown in Fig. 2 for $\beta_e = 10$, 15, and 20. Substituting (4) into (7), we find that the critical loads for the sway and nonsway buckling modes coincide if the bracing has a certain critical stiffness characterized by

$$\beta_e = \lambda^3 \left(\lambda - \frac{3 \sin \lambda}{2 + \cos \lambda}\right)^{-1} \tag{9}$$

If β_b is given, λ needs to be solved from the transcendental equation (4) (e.g., by Newton's iterative method), and then the corresponding critical bracing stiffness parameter β_e can be evaluated from (9). To get the plot of β_e versus β_b, it is simpler

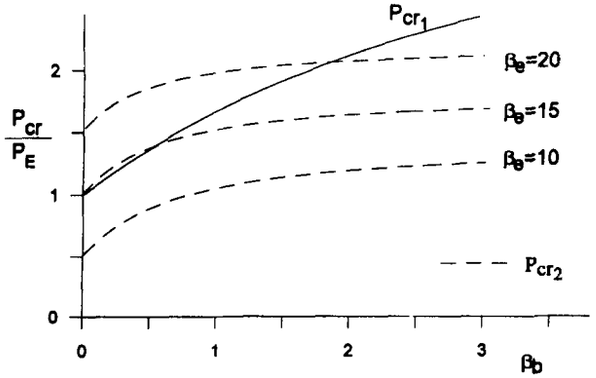

FIG. 2. Critical Loads versus Bracing Stiffness

to choose a series of values of λ and for each of them evaluate β_b from (4) and β_e from (9).

INITIAL POSTCRITICAL BUCKLING ANALYSIS

The postcritical behavior is a geometrically nonlinear problem. However, we are interested only in the initial postcritical behavior, for which only one order of accuracy above that of the linearized theory of buckling is needed. The cause of nonlinearity is that the dependence of the curvature on the deflection slope is nonlinear and the dependence of the axial shortening on the deflection slope is a higher than quadratic function. A differentiation generally decreases the accuracy of approximation of a curve by one order. Vice versa, integration increases the order of accuracy by one order. Therefore, if we take the distribution of θ according to the linearized theory of buckling, which is sinusoidal and only first-order accurate, and integrate θ with at least a second-order accuracy to obtain the deflections, the deflections will be second-order accurate in terms of the rotations, and thus sufficient for the purpose of initial postcritical analysis.

Therefore, it is possible to assume the same distribution of rotation $\theta(x)$ along the column as in the classical linearized theory, i.e., the sinusoidal distribution (even though the exact distribution of $\theta(x)$ at large deflections is not sinusoidal). The potential energy depends quadratically on the curvatures and linearly on the axial shortening. Therefore, it is necessary to express the curvatures from the rotations with at least second-order accuracy in terms of the rotations, and the axial shortening with at least fourth-order accuracy in terms of the rotations. This approach was proposed in section 5.9 of Bažant and Cedolin (1991) and it was demonstrated that it gives correct results for a column.

To integrate the rotations with second-order accuracy, instead of the rectilinear axial coordinate x it is now better to use the curved length coordinate s of the deflected column; s is measured from the column midheight along the deflection curve [Fig. 1(c, e)]. The distribution of θ according to the linear theory is a general linear combination of the expressions in (2) and (6). Because this distribution needs to be only first-order accurate, we may replace x with s, and so we introduce

$$\theta(s) = \theta_0(\xi) + q_1 \sin \lambda\xi + q_2 \cos \lambda\xi + q_3,$$

$$\text{with} \quad \theta_0(s) = \alpha_1 \sin \pi\xi + \alpha_2 \tag{10}$$

in which $\xi = s/l_c$ = dimensionless coordinate along the curve; q_1, q_2, and q_3 = generalized displacements. The initial slope $\theta_0(\xi)$ represents the initial imperfection of the column, assumed also as sinusoidal: α_1, α_2 are the given initial imperfection parameters, of which α_1 represents the amplitude of the symmetric (sinusoidal) imperfection of the column and α_2 represents the amplitude of the initial asymmetric imperfection (sway angle of the floor). From (10)

$$\frac{\partial\theta}{\partial\xi} = \frac{\partial\theta_0}{\partial\xi} + \lambda(q_1 \cos\lambda\xi - q_2 \sin\lambda\xi), \quad \frac{\partial\theta_0}{\partial\xi} = \pi\alpha_1 \cos\pi\xi \tag{11}$$

The curvature is exactly $\partial\theta/\partial s$, and so the energy expressions in (1) can be written as

$$U_c = \int_{-l_c/2}^{l_c/2} \frac{EI_c}{2}\left(\frac{\partial\theta}{\partial s} - \frac{\partial\theta_0}{\partial s}\right)^2 ds = \int_{-1/2}^{1/2} \frac{EI_c}{2l_c}\left(\frac{\partial\theta}{\partial\xi} - \frac{\partial\theta_0}{\partial\xi}\right)^2 d\xi \tag{12}$$

$$U_b = \frac{2EI_b}{l_b}\left[3\left(q_3 + q_2 \cos\frac{\lambda}{2}\right)^2 + 2q_1^2 \sin^2\frac{\lambda}{2}\right] \tag{13}$$

$$U_e = \frac{C_b}{2}\Delta^2, \quad W = Pu_1 \tag{14}$$

where u_1 = axial shortening of the whole column; and Δ = horizontal relative displacement between the top and bottom of the column. Their exact expressions in terms of $\theta(s)$ are

$$u_1 = \int_{-l_c/2}^{l_c/2} (\cos\theta_0 - \cos\theta)\, ds = l_c \int_{1/2}^{1/2} (\cos\theta_0 - \cos\theta)\, d\xi \tag{15}$$

$$\Delta = \int_{-l_c/2}^{l_c/2} \sin\theta\, ds = l_c \int_{-1/2}^{1/2} \sin\theta\, d\xi \tag{16}$$

The nonlinearity of the foregoing expression arises from the use of the curved coordinate s instead of the rectilinear axial coordinate x, and from functions $\cos\theta$ and $\sin\theta$. These functions cannot be approximated as $\cos\theta = 1 - (\theta^2/2)$, $\sin\theta = \theta$ because that would yield a linearized theory, insufficient for postcritical analysis. For this reason, an explicit expression for the potential energy Π is impossible, but it is also unnecessary.

The equilibrium equations are $\partial\Pi/\partial q_1 = 0$, $\partial\Pi/\partial q_2 = 0$, $\partial\Pi/\partial q_3 = 0$. Substituting (1), we have the conditions

$$\frac{\partial U}{\partial q_1} - P\frac{\partial u_1}{\partial q_1} = 0, \quad \frac{\partial U}{\partial q_2} - P\frac{\partial u_1}{\partial q_2} = 0, \quad \frac{\partial U}{\partial q_3} - P\frac{\partial u_1}{\partial q_3} = 0 \tag{17}$$

in which

$$\frac{\partial U}{\partial q_1} = \frac{EI_c}{2l_c}\left[\lambda(\lambda + \sin\lambda)q_1 + 2\beta_e\Delta I_1 + 8\beta_b q_1 \sin^2\frac{\lambda}{2}\right] \tag{18a}$$

$$\frac{\partial U}{\partial q_2} = \frac{EI_c}{2l_c}\left[\lambda(\lambda - \sin\lambda)q_1 + 2\beta_e\Delta I_2 + 24\beta_b\left(q_2 \cos\frac{\lambda}{2} + q_3\right)\cos^2\frac{\lambda}{2}\right] \tag{18b}$$

$$\frac{\partial U}{\partial q_3} = \frac{EI_c}{l_c}\left[\beta_e\Delta I_3 + 12\beta_b\left(q_2 \cos\frac{\lambda}{2} + q_3\right)\right] \tag{18c}$$

$$\frac{\partial u_1}{\partial q_1} = l_c \int_{-1/2}^{1/2} \sin\theta \sin\lambda\xi\, d\xi = l_c I_4 \tag{19a}$$

$$\frac{\partial u_1}{\partial q_2} = l_c \int_{-1/2}^{1/2} \sin\theta \cos\lambda\xi\, d\xi = l_c I_5 \tag{19b}$$

$$\frac{\partial u_1}{\partial q_3} = l_c \int_{-1/2}^{1/2} \sin\theta\, d\xi = l_c I_6 \tag{19c}$$

with the notations

$$I_1 = \int_{-1/2}^{1/2} \cos\theta \sin\lambda\xi\, d\xi, \quad I_2 = \int_{-1/2}^{1/2} \cos\theta \cos\lambda\xi\, d\xi,$$

$$I_3 = \int_{-1/2}^{1/2} \cos\theta\, d\xi \tag{20}$$

The equation system (17) is nonlinear, and a numerical solution is necessary. An effective method of solution is the Levenberg-Marquardt optimization algorithm (available as a standard library subroutine). In nonlinear problems, the objective function to be minimized, representing the sum of squares of the right-hand sides of the nonlinear equations, has many local minima. For this reason, the solution of nonlinear problems is difficult. The optimization algorithm often converges to some incorrect local minimum.

The present problem, however, belongs to a special class of nonlinear problems for which the solution is easy because a good initial estimate of the solution can always be supplied to the optimization subroutine. This is the special class of problems for which the evolution of the solution depending on some control parameter can be traced in small steps from a simple initial state. We solve a sequence of problems such that the input values change from one problem to the next only sufficiently little, in which case the solution of the previous problem provides a good initial estimate for the next problem.

For a given value of load P, several different solutions may exist because of interactions between different modes of buckling. The multiplicity of solutions is especially marked when P is close to the critical load or the maximum load. The values of q_1, q_2, and q_3 are then very sensitive to P. A very small increment of load P may cause large increments of q_1, q_2, and q_3, and sometimes no solution can be found. Furthermore, when P is the controlled variable, the tangential stiffness matrix is nearly singular in the vicinity of the maximum load, which induces instability of numerical solution. Therefore, setting the P value as the input would not be a wise procedure. It is better to specify q_1 (or q_2) as the input and then solve for P, q_3, and q_2 (or q_1). In that case, load control is replaced by displacement control of q_1 (or q_2), and consequently [see e.g., Bažant and Cedolin (1991), chapter 4], the structure becomes stable at the maximum load and even for a certain range beyond the maximum load until a snapback state is reached (if ever). Stability of the structures ensures stability of the present numerical solution. Whether it is better to set the value of q_1 or of q_2 as the input depends on which critical mode dominates. Gaining some experience helps.

The integrals in (18)–(20) are evaluated by numerical quadrature (an eight-point Gaussian quadrature was used). When q_1, q_2, q_3, α_1, α_2 are so small that their maximum is less than 0.05, the following integrals may be approximated by the expression based on the linearized theory

$$\Delta \approx [2q_2 \sin(\lambda/2) + q_3\lambda]l_c/\lambda \tag{21}$$

$$I_4 \approx \alpha_1\left[\frac{\sin(\pi - \lambda)/2}{\pi - \lambda} - \frac{\sin(\pi + \lambda)/2}{\pi + \lambda}\right] + q_1\frac{\lambda - \sin\lambda}{2\lambda} \tag{22}$$

$$I_5 \approx [q_2(\lambda + \sin\lambda) + 4(q_3 + \alpha_2)\sin(\lambda/2)]/\lambda \tag{23}$$

$$I_6 \approx [2q_2/\lambda \sin(\lambda/2)] + q_3 + \alpha_2 \tag{24}$$

POSTCRITICAL BEHAVIOR AND IMPERFECTION SENSITIVITY

Frames with various stiffness parameters β_b and β_e and various imperfections have been analyzed. As before, the critical loads for the nonsway (symmetric) and sway (nonsymmetric) buckling modes of the perfect structure are denoted as P_{cr_1} and P_{cr_2}, respectively. The numerical results are plotted in Figs. 3(a, b)–10(a, b), which show the plots of the load P versus the load-point displacement u_1 (the axial shortening of the column), and of the load P versus the lateral deflection w_0 of column at midheight, for various values of imperfection parameters $\alpha = \alpha_1$ and α_2, including the case of no imperfection (perfect structure). The plots of maximum postcritical load P_{max} versus the imperfection parameter $\alpha = \alpha_1$ or α_2, called the imperfection sensitivity diagrams, are also given [Figs. 3(c), 4(c), 5(c), 7(c), 8(c), and 9(c)]. The value of w_0 is calculated as

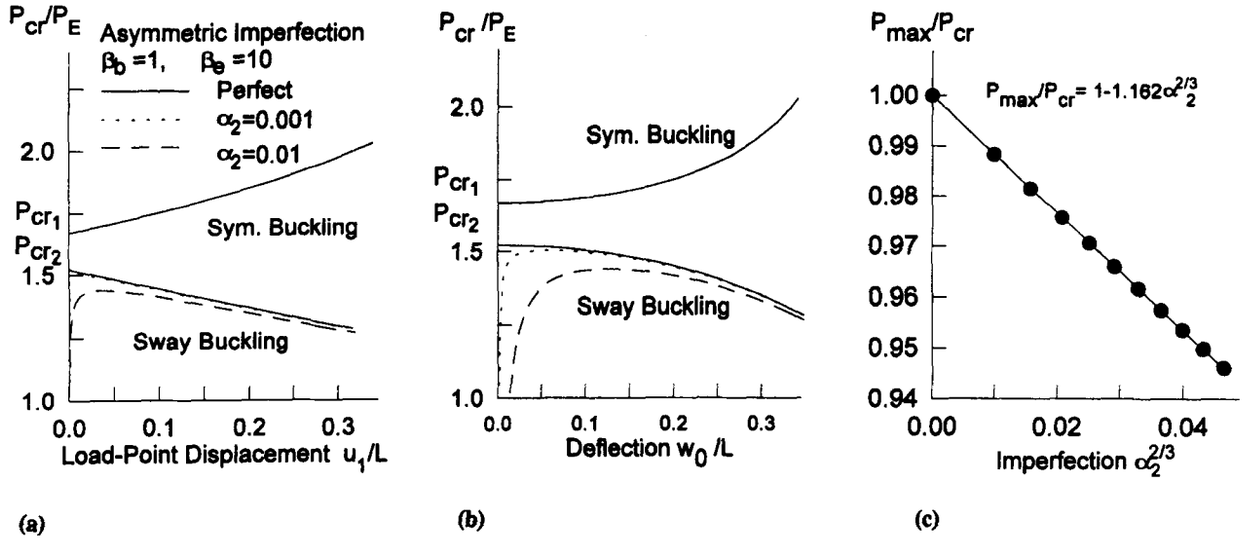

FIG. 3. Sway Buckling of Imperfect Frame for $P_{cr_1} > P_{cr_2}$: (a) Load-Point Displacement; (b) Midspan Deflection; (c) Imperfection Sensitivity

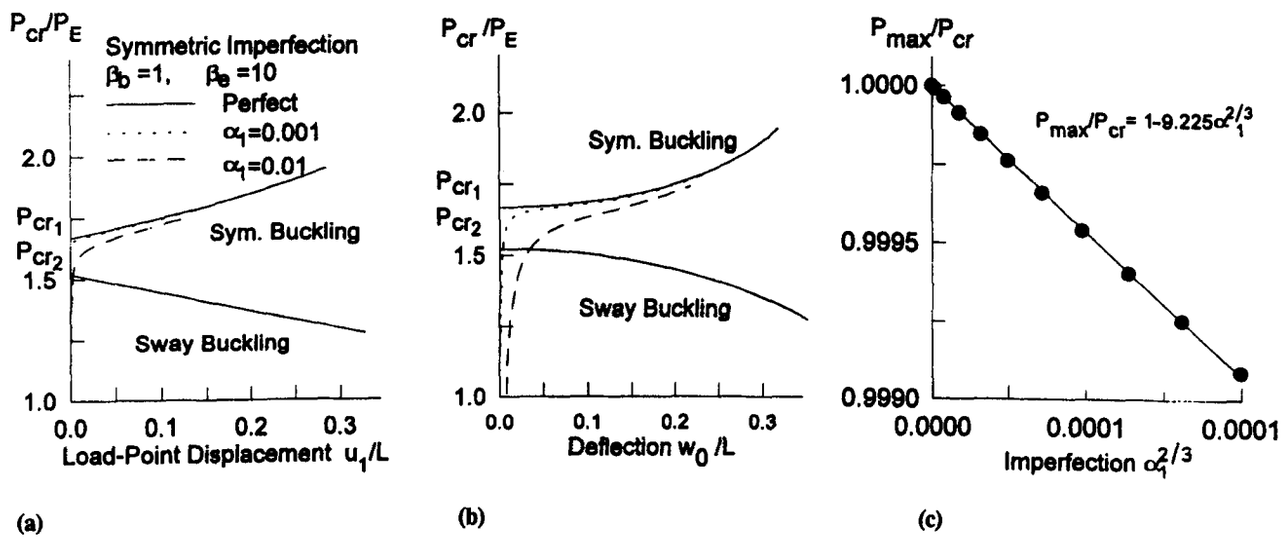

FIG. 4. Symmetric Buckling of Imperfect Frame for $P_{cr_1} > P_{cr_2}$: (a) Load-Point Displacement; (b) Midspan Deflection; (c) Imperfection Sensitivity

$$w_0 = \int_{-l_c/2}^{0} \sin\theta \, ds = l_c \int_{-1/2}^{0} \sin\theta \, d\xi \tag{25}$$

As seen from Figs. 3(a, b)–10(a, b), calculations are made only for what can be expected the most dangerous imperfections—either the asymmetric imperfection of the symmetric imperfection, but not both simultaneously. Of course calculations could have been run for various combinations of these imperfections. But that would greatly expand the number of plots to show, and would also complicate the interpretation based on the fitting of Koiter's power law to the maximum load values. However, the fact that the load-deflection diagrams for one imperfection lie far above the load-deflection diagrams for the other imperfection (as seen by comparing, e.g., Figs. 3 and 4) suggests that combined imperfections can hardly be expected to interact strongly, and so their consideration is probably unimportant. This should nevertheless be checked in future studies. In any case, though, the simultaneous effect of combined symmetric and asymmetric imperfections could not make the imperfection sensitivity weaker, and so it is certain that the imperfection sensitivity is at least as strong as shown here.

The symmetric and asymmetric imperfection shapes are chosen in (10) as simple shapes. Other shapes may be expected to give similar results. The important point is that the deflection according to the symmetric (or asymmetric) shape does work on the first symmetric (or asymmetric) buckling mode. This guarantees the chosen imperfections to excite both buckling modes.

The diagrams of P versus w_0 are the conventional plots. Unlike these diagrams, the diagrams of P versus u_1 make it possible to decide stability of equilibrium states because P is conjugated by work with u_1; when the load is a dead load (gravity load), a rising (or descending) diagram $P(u_1)$ implies a stable (or unstable) state [see e.g., Bažant and Cedolin (1991), chapter 10]. Based on the numerical results shown, the following observations can be made.

All the plots of P versus u_1 or w_0 show that the postcritical behavior of the frame is always of the type called symmetric bifurcation. The asymmetric bifurcation, which is always unstable and has a stronger imperfection sensitivity, never occurs.

The bifurcations in Fig. 9(a, b), with a rising postbifurcation branch, are of the stable type. They are known to be imperfection insensitive. The bifurcations in Figs. 3(a, b) and 5(a,

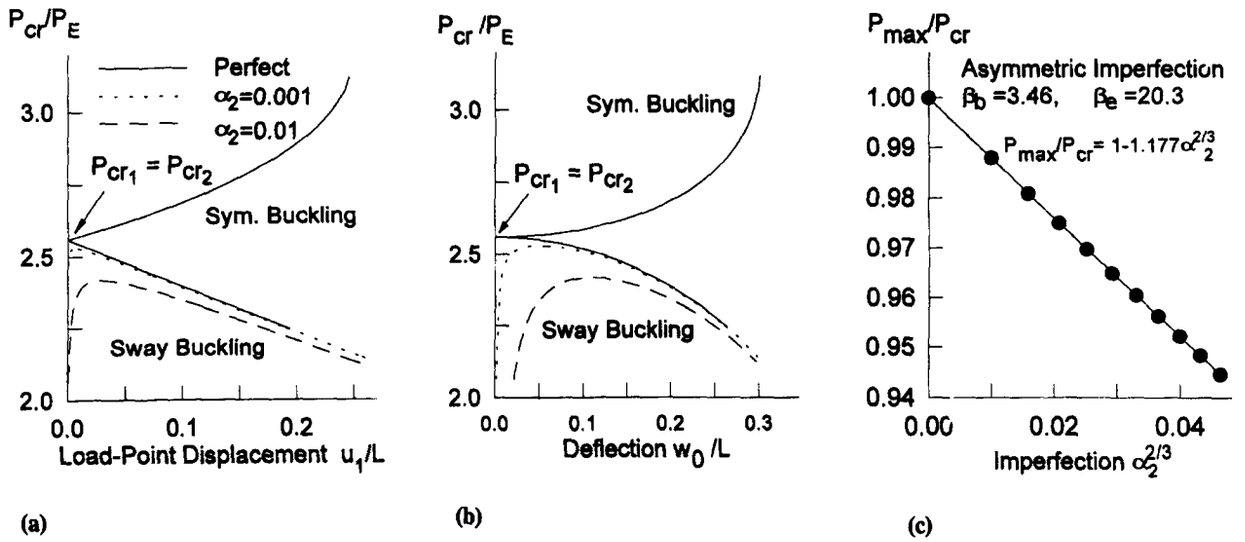

FIG. 5. Sway Buckling of Imperfect Frame for $P_{cr_1} = P_{cr_2}$: (a) Load-Point Displacement; (b) Midspan Deflection; (c) Imperfection Sensitivity

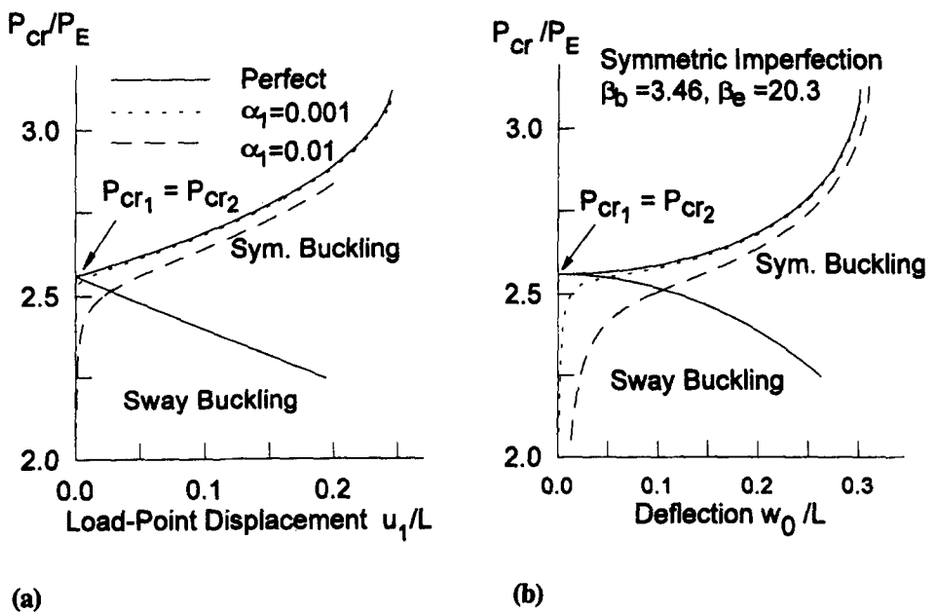

FIG. 6. Symmetric Buckling of Imperfect Frame for $P_{cr_1} = P_{cr_2}$: (a) Load-Point Displacement; (b) Midspan Deflection

b), with a descending postbifurcation branch, are of the unstable type, known to be imperfection sensitive and to follow Koiter's 2/3-power law which states that

$$P_{max} = P_{cr}[1 - (\alpha/\alpha_0)^{2/3}] \tag{26}$$

where α_0 = constant [see, e.g., Bažant and Cedolin (1991), sections 4.3–4.6]. The imperfection sensitivity of the postcritical maximum load P_{max} is seen in Figs. 3(c) and 5(c), and Koiter's 2/3-power law is confirmed by the fact that the plot of P_{max} versus $\alpha^{2/3}$ is a straight line initially (for very large deflections it cannot be a straight line). The imperfection sensitivity is always associated with the sway mode of postcritical buckling of the frame.

The imperfection sensitivity is seen to occur only when $P_{cr_1} \geq P_{cr_2}$, i.e., when the bracing is sufficiently soft or nonexistent. The cases $P_{cr_1} < P_{cr_2}$ are never imperfection-sensitive except when both critical loads are too close to each other. In this regard it may be noted that the equilibrium load-deflection diagrams in Figs. 8(b) and 9(b) exhibit a decrease of their peak load with increasing imperfection, but this is practically irrelevant because these diagrams are not associated with the lowest critical load; they do not represent stable states and are not realizable in a normal loading process.

When two critical modes coincide, the imperfection sensitivity often becomes stronger, either in terms of the amplitude coefficient α_0 or also in terms of the exponent of α. Fig. 5 shows the load-deflection diagrams for sway (asymmetric) imperfections of various magnitudes. For bracing such that $P_{cr_1} = P_{cr_2}$, the imperfection sensitivity is indeed seen to be slightly stronger but only in terms of the amplitude rather than in terms of the exponent of α in Koiter's power law. The reason that the exponent does not change from $-2/3$ to $-1/2$ is that one of the two critical loads is associated with stable, imperfection insensitive, bifurcation. (For this reason, it is unnecessary to show here the load-deflection diagrams when a combined sway and non-sway imperfection is present.)

Fig. 7 shows that, practically, the imperfection sensitivity persists even when P_{cr_1} is slightly smaller than P_{cr_2}, i.e., when $P_{cr_1} = P_{cr_2} - \delta$ where δ is a small positive number ($\delta << P_{cr_1}$). For this reason, there should be a certain margin against

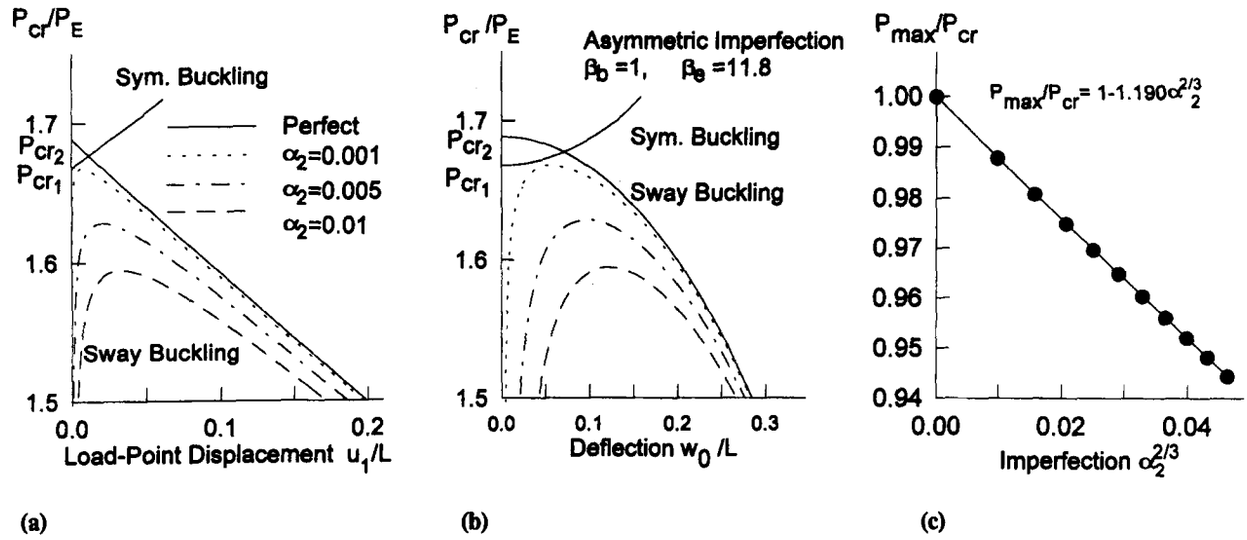

FIG. 7. Sway Buckling of Imperfect Frame for $P_{cr_1} = P_{cr_2} - \delta$: (a) Load-Point Displacement; (b) Midspan Deflection; (c) Imperfection Sensitivity

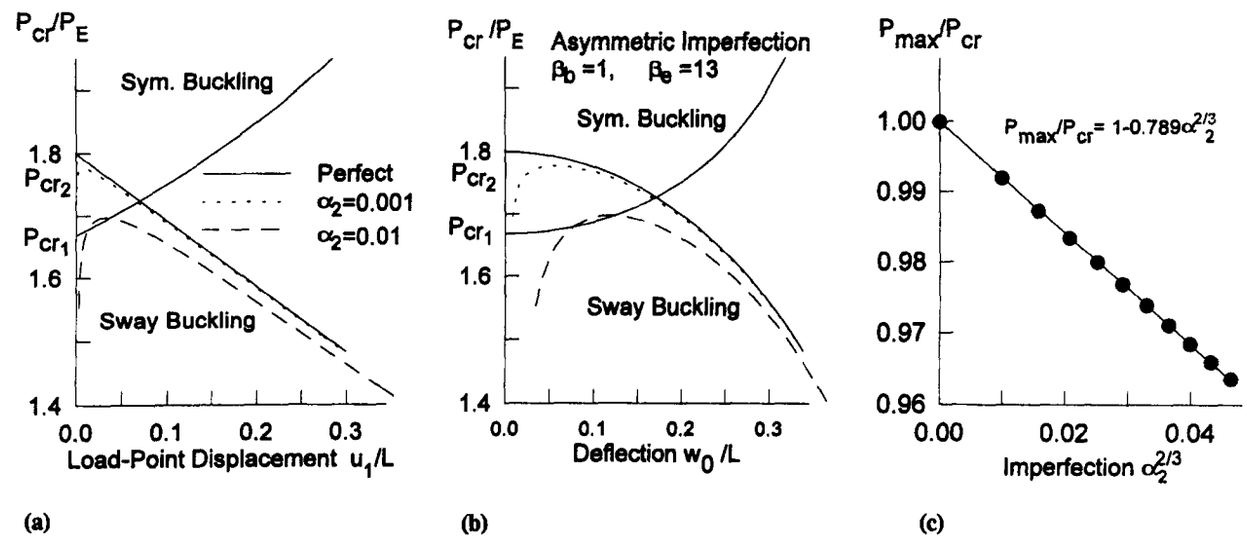

FIG. 8. Sway Buckling of Imperfect Frame for $P_{cr_1} < P_{cr_2}$: (a) Load-Point Displacement; (b) Midspan Deflection; (c) Imperfection Sensitivity

the occurrence of the case for which the sway and nonsway critical loads coincide.

As revealed by Figs. 5 and 6, the magnitude of the decrease of maximum load caused by the imperfection sensitivity for imperfection $\alpha = 0.01$ is approximately 5.7% when both critical loads coincide or nearly coincide. However, this is roughly the minimum imperfection to consider in the design of columns (the ACI code actually prescribed the minimum eccentricity of the axial load on a column to be considered as 1% of the column length). Much larger eccentricities can be caused by bending moments applied at the ends of a column, for example the moments caused by asymmetric loads on the floors of buildings or by the wind. For such large eccentricities the present initial postcritical analysis is probably insufficient and higher-order terms may have to be included in the analysis. Nevertheless, it is clear that in such cases the imperfection sensitivity of buckling, if it occurs, can reduce the maximum load as much as 15%.

The plot of β_e versus β_b for the case $P_{cr_1} = P_{cr_2}$ is given in Fig. 11. For this case, the bracing design according to the usual analysis ignoring the postcritical behavior appears optimal in the use of material. But it is in fact the so-called naive optimal design.

A design that is truly optimal from the viewpoint of buckling (considered alone) is that for which the critical loads for the symmetric and asymmetric buckling are as close as possible but not so close as to produce a significant imperfection sensitivity. This requires a certain safety factor $\mu_{opt} > 1$ against the case of naively optimal bracing occurring for $P_{cr_1} = P_{cr_2}$ (from experience with other similar problems, the value μ_{opt} is likely to be somewhere between 1.1 and 2, and will depend on the severity of the imperfection). Therefore, the (nonnaive) optimal bracing is characterized by

$$[\beta_e]_{opt} = \mu_{opt}\lambda^3 \left(\lambda - \frac{3 \sin \lambda}{2 + \cos \lambda}\right)^{-1} \tag{27}$$

Bracing softer than this should never be used. If β_b is given, λ first needs to be solved from the transcendental equation (4) (e.g., by Newton's iterative method), and then the corresponding truly optimal bracing stiffness parameter $[\beta_e]_{opt}$ can be evaluated from (27). To get the plot of $[\beta_e]_{opt}$ versus β_b, it is simpler to choose a series of values of λ and for each of them evaluate β_b from (4) and $[\beta_e]_{opt}$ from (9).

On the other hand, bracing much stiffer than that given by

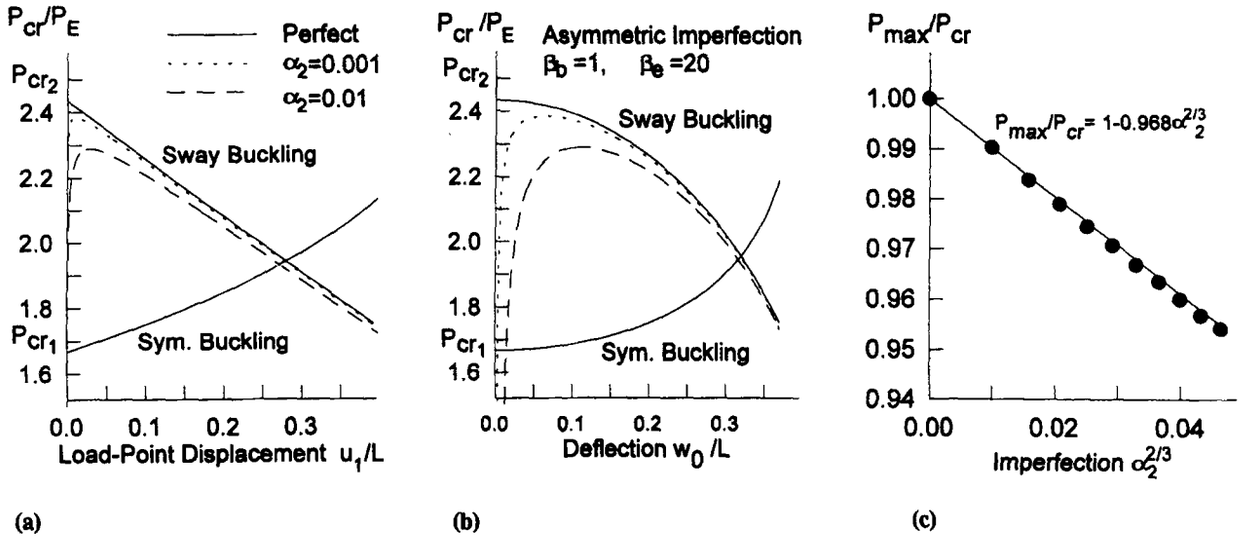

FIG. 9. Sway Buckling of Imperfect Frame for $P_{cr_1} << P_{cr_2}$: (a) Load-Point Displacement; (b) Midspan Deflection; (c) Imperfection Sensitivity

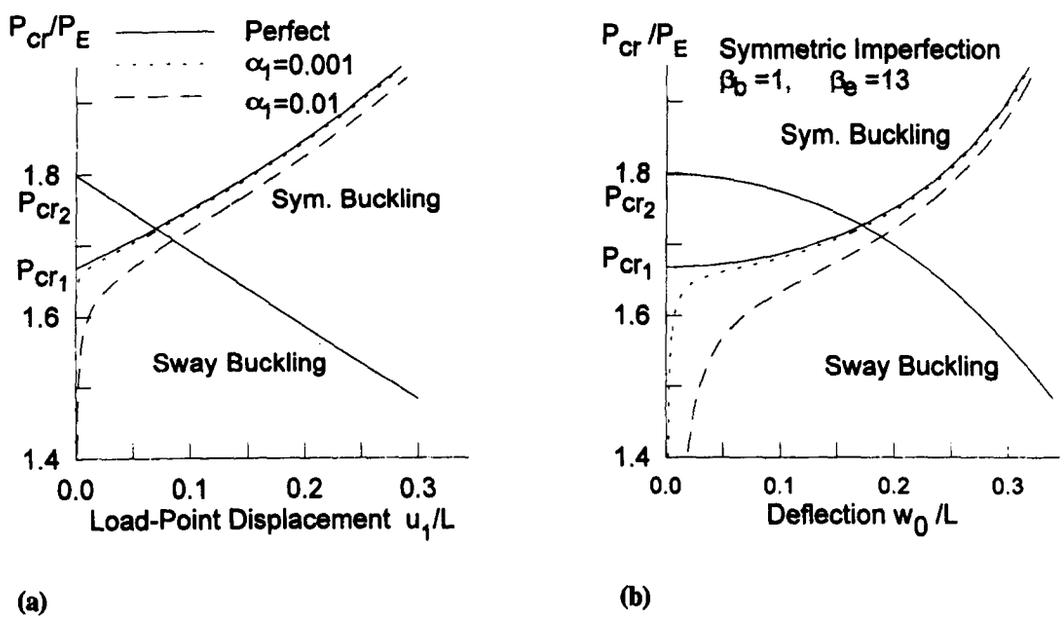

FIG. 10. Symmetric Buckling of Imperfect Frame for $P_{cr_1} < P_{cr_2}$: (a) Load-Point Displacement; (b) Midspan Deflection

(27) is uneconomical from the viewpoint of buckling (although it might be needed to resist wind and earthquake).

When a symmetric imperfection with $P_{cr_1} < P_{cr_2}$ is considered, the present calculation method yields the load-deflection diagrams exemplified in Fig. 10. It is interesting that the load-deflection diagram for an imperfect structure, as well as that obtained for the limit case of a perfect structure (or a structure with an extremely small imperfection), exhibits a bifurcation such that the bifurcation point and the descending bifurcated branch lie above the descending load-deflection diagram for postcritical buckling of the perfect structure in the sway mode. However, states above this diagram cannot be stable and are not reachable by a normal loading process. Such results of calculations must be fictitious. They are doubtless obtained as a consequence of the fact that the distribution of rotation along the column is here restricted to be sinusoidal (and thus free of nonsinusoidal types of imperfections).

The maximum load of a frame with high imperfection sensitivity is reached only at rather large deflections—approximately $w_0 = 0.1L$ for imperfection $\alpha_2 = 0.01$ according to Fig. 5(b). At such a large deflection, practical frames are likely to develop inelastic response. Its consideration is recommended for future studies. The inelastic response of the imperfect frame at large deflections is likely to reduce further the maximum load compared to the critical load of elastic frame, and so it can only increase the imperfection sensitivity. Also, the initial postcritical analysis may become too inaccurate at such large deflections and higher-order terms may have to be considered.

Similar conclusions may be obtained for other frames, e.g., the portal frame. For that frame, the effect of the bracing stiffness on the critical loads for the sway and nonsway modes was studied by Kounadis (1983). He determined the bracing stiffness for which both critical loads coincide. Knowing from the investigations of Kounadis (1980) and Simitses et al. (1981) that the sway buckling mode for that frame, same as for our frame, is imperfection sensitive, and the nonsway buckling mode insensitive, Kounadis (1983) proposed that the bracing must be stiffer than that for which both buckling modes coincide, although he did not speculate how much stiffer.

Similarly, one could derive the conditions of the optimum

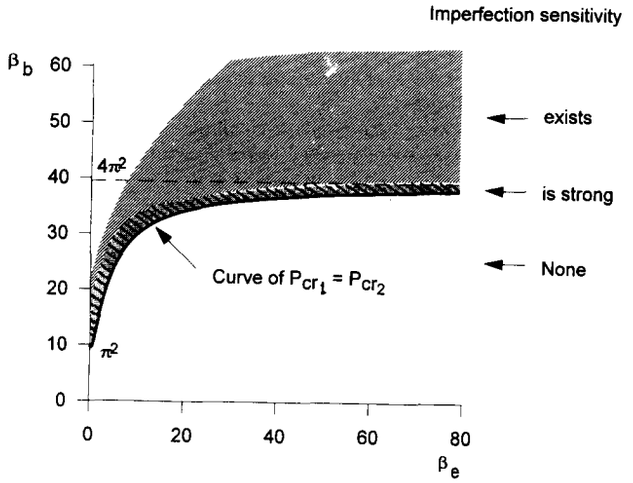

FIG. 11. Imperfection Sensitivity Regions

bracing design (1) for the buckling of boundary columns of a large regular frame; (2) for the interior buckling and boundary column buckling of an infinite one-story multibay regular frame; (3) for the interior buckling and boundary column buckling for the top floor in an infinite multistory multibay regular frame; and (4) for the interior or top-floor buckling of a one-bay multistory regular frame. In the cases of boundary columns, the buckling mode is not periodic but exponentially decaying into the interior of the frame. The problem is then coupled to difference equations of a type similar to equation 2.4.8 of Bažant and Cedolin (1991).

CONCLUSIONS

1. The periodic interior buckling of a large regular multibay multistory rectangular frame with elastic bracing involves both nonsway (symmetric) and sway (antisymmetric) modes as the first two buckling modes. There exists a certain critical bracing stiffness such that the critical loads for the nonsway and sway modes coincide. Simple formulae for this critical stiffness are given.
2. For this and softer bracing, the postcritical buckling behavior is of the type of unstable symmetric bifurcation which exhibits imperfection sensitivity following Koiter's 2/3-power law. Such bracing stiffness should be avoided in design. For stiffer bracing, there is no imperfection sensitivity.
3. From the viewpoint of critical loads alone, the bracing for which the critical loads for the sway and nonsway modes coincide may seem optimal. But it represents the so-called naive optimal design, because the imperfection sensitivity is the strongest in this case. It is recommended that the bracing that is truly optimal from the viewpoint of buckling should be sufficiently stiffer (perhaps 50% stiffer) than the bracing for which both critical loads coincide. In that case the frame exhibits stable symmetric bifurcation and there is no imperfection sensitivity.
4. The buckling behavior, including the postcritical imperfection sensitivity, is similar to that of a portal frame analyzed by Simitses et al. (1981) and Kounadis (1983).
5. A recently proposed simple method for the initial postcritical analysis of frames (Bažant and Cedolin 1991) is demonstrated. In this method, one assumes the distribution of cross section rotations along the columns and beams to be the same as in the buckling modes of the perfect frame (obtained by the classical linearized theory of buckling, which gives a sinusoidal distribution if the cross section is uniform). Then the curvatures and deflections are obtained from the rotations by integration with at least a second-order accuracy in terms of the rotations, and the axial shortening with at least a third-order accuracy. A potential energy expression (which is fourth-order accurate in terms of deflections, axial shortening, and curvatures) is thus obtained and minimized.

APPENDIX I. LINEARIZED BUCKLING ANALYSIS BY ENERGY MINIMIZATION

For small deflections,

$$U_c = \int_0^{l_c} \frac{EI_c}{2}(w_c'')^2\,dx, \quad U_b = \int_0^{l_b} \frac{EI_b}{2}(w_b'')^2\,dx, \quad U_e = \frac{1}{2}C_b\Delta^2 \tag{28}$$

$$W = Pu_1 = P\int_0^{l_c} \frac{1}{2}(w_c')^2\,dx \tag{29}$$

Since the initial axial force in the beam is zero and its increment caused by buckling is second-order small and thus negligible, the elementary theory of bending applies to the beam. Therefore, according to the well-known stiffness matrix of a beam without axial force

$$U_b = \frac{2EI_b}{l_b}(\theta_1^2 + \theta_2^2 + \theta_1\theta_2) \tag{30}$$

Nonsway Buckling Mode

Substituting (2) and $\theta = qk\cos(\lambda/2)$ into (28)–(30), we get

$$U_c = 0.25EI_c k^3 q^2(\lambda + \sin\lambda), \quad U_b = 2EI_b l_b^{-1}k^2q^2\cos^2(\lambda/2),$$

$$U_e = 0 \tag{31}$$

$$W = 0.25Pkq^2(\lambda - \sin\lambda) \tag{32}$$

The equilibrium condition is $\partial\Pi/\partial q = 0$, which yields

$$P = \pi^{-2}P_E\lambda[\lambda(\lambda + \sin\lambda) + 8\beta_b\sin^2(\lambda/2)](\lambda - \sin\lambda)^{-1} \tag{33}$$

Substituting further (3) into (33), we get the condition in (4) for the critical load for nonsway buckling.

Sway Buckling Mode

Expressing the end rotations θ_1, θ_2 and column top displacement Δ from (6), and substituting them along with (6) into (28)–(30), we get

$$U_c = 0.25EI_c k^3 q_1^2(\lambda - \sin\lambda), \quad U_b = 6EI_b l_b^{-1}[kq_1\cos(\lambda/2) + q_3]^2 \tag{34}$$

$$U_e = 0.5C_b[2q_1\sin(\lambda/2) + q_3]^2 \tag{35}$$

$$W = 0.25Pl_c^{-1}[q_1^2\lambda(\lambda + \sin\lambda) + 2q_3^2 + 8q_1q_3\sin(\lambda/2)] \tag{36}$$

Equilibrium requires that $\partial\Pi/\partial q_1 = 0$ and $\partial\Pi/\partial q_3 = 0$. This yields a system of two homogeneous linear equations for two unknowns q_1 and q_3. A nonzero solution is possible if and only if the determinant of this equation system vanishes. This leads to the quadratic equation $a_0P^2 - a_1P + a_2 = 0$ in which

$$a_0 = \lambda(\lambda + \sin\lambda) - 8\sin^2(\lambda/2) \tag{37}$$

$$a_1 = EI_c l_c^{-2}\{12\beta_b[\lambda^2(2 + \cos\lambda) - 3\lambda\sin\lambda] + \beta_e[\lambda^2 + \lambda\sin\lambda - 8\sin^2(\lambda/2)] + \lambda^3(\lambda - \sin\lambda)\} \tag{38}$$

$$a_2 = EI_c l_c^{-4}\{12\beta_b\lambda^3(\lambda - \sin\lambda) + \beta_e\lambda^3(\lambda - \sin\lambda) + 24\beta_b\beta_e[\lambda\cos(\lambda/2) - 2\sin(\lambda/2)]^2\} \tag{39}$$

Solving this quadratic equation with (37)–(39), we obtain the condition in (7) for the critical load for sway buckling.

APPENDIX II. REFERENCES

Bažant, Z. (1943). "Buckling strength of frame structures." *Technický Obzor*, Prague, Czechoslovakia, 51(7, 8, and 16) (in Czech).

Bažant, Z. P., and Cedolin, L. (1989). "Initial postcritical analysis of asymmetric bifurcation in frames." *J. Engrg. Mech.*, ASCE, 115(11), 2845–2857.

Bažant, Z. P., and Cedolin, L. (1991). *Stability of structures: elastic, inelastic, fracture and damage theories*. Oxford University Press, New York, N.Y.

Bleich, F. (1961). *Buckling strength of metal structures*. McGraw-Hill Book Co., New York, N.Y.

Britvec, S. J. (1973). *The stability of elastic systems*. Pergamon Press, Inc., New York, N.Y.

Brush, D., and Almroth, B. O. (1975). *Buckling of bars, plates and shells*. McGraw-Hill Book Co., New York, N.Y.

Budianski, B. (1974). "Theory of buckling and post-buckling behavior of structures." *Advances in Applied Mechanics*, C. S. Yih, ed., Academic Press, Inc., San Diego, Calif., 1–65.

Chwalla, E. (1938). "Die Stabilität lotrecht belasteter Rechteckrahmen." *Bauingenieur*, 19, 69.

Hutchinson, J. W., and Koiter, W. T. (1970). "Postbuckling theory." *ASME Appl. Mech. Rev.*, 23(12), 1353–1366.

Koiter, W. T. (1945). "Over de stabiliteit van het elastische evenwicht," dissertation, Delft, Holland, The Netherlands (in Dutch).

Koiter, W. T. (1967). "Post-buckling analysis of simple two-bar frame." *Recent progress in applied mechanics*, B. Broberg et al., eds., (Folke Odqvist Volume), Almqvist & Wiksells, Stockholm, Sweden, 337 (Section 2.6).

Koiter, W. T., and Kuiken, G. D. C. (1971). "The interaction between local buckling and overall buckling and the behavior of built-up columns." *Rep. No. 447*, Lab. of Engrg. Mech., Delft Univ. of Technol., Delft, The Netherlands.

Kollár, L., and Dulácska, E. (1984). *Buckling of shells for engineers*. John Wiley & Sons, Inc., New York, N.Y.

Kounadis, A. N. (1983). "Interaction of the joint and of the lateral bracing stiffnesses for the optimum design of unbraced frames." *Acta Mechanica*, 47, 247–262.

Kounadis, A. N. (1985). "An effective simplified approach for the nonlinear buckling analysis of frames." *AIAA J.*, 23(8), 1254–1259.

Kounadis, A. N., Giri, J., and Simitses, G. J. (1977). "Nonlinear stability analysis of an eccentrically loaded two-bar frame." *J. Appl. Mech.*, 44(4), 701–706.

Roorda, J. (1965a). "Stability of structures with small imperfections." *J. Engrg. Mech.*, ASCE, 91(1), 87–106.

Roorda, J. (1965b). "The instability of imperfect elastic structures." PhD dissertation, Univ. of London, England.

Roorda, J. (1968). "On the buckling of symmetric structural systems with first and second order imperfections." *Int. J. Solids and Struct.*, 4, 1137–1148.

Roorda, J., and Chilver, A. M. (1970). "Frame buckling: an illustration of the perturbation technique." *Int. J. Non-Linear Mech.*, 5, 235–246.

Simitses, G. J. (1976). *An introduction to the elastic stability of structures*. Prentice-Hall, Inc., Englewood Cliffs, N.J.

Simitses, G. J., Giri, J., and Kounadis, A. N. (1981). "A nonlinear analysis of portal frames." *Int. J. for Numer. Methods in Engrg.*, 17, 123–132.

Thompson, J. M. T., and Hunt, G. W. (1984). *Elastic instability phenomena*. John Wiley & Sons, Inc., London, England.

Timoshenko, S. P., and Gere, J. M. (1961). *Theory of elastic stability*, 2nd Ed., McGraw-Hill Book Co., Inc., New York, N.Y., Sec. 2.1.

von Mises, R., and Ratzendorfer, J. (1926). "Die Knicksicherheit von Rahmentragwerken." *Zeitschrift für Angew. Math. und Mech. (ZAMM)*, Germany, 6, 181.